

Article

Enhanced Crystal Quality of $\text{Al}_x\text{In}_{1-x}\text{As}_y\text{Sb}_{1-y}$ for Terahertz Quantum Cascade Lasers

Tobias Zederbauer ^{1,*}, Aaron Maxwell Andrews ¹, Donald MacFarland ¹, Hermann Detz ², Werner Schrenk ³ and Gottfried Strasser ^{1,3}

¹ TU Wien, Institute of Solid State Electronics, Floragasse 7, 1040 Wien, Austria; aaron.andrews@tuwien.ac.at (A.M.A.); donald.macfarland@tuwien.ac.at (D.M.); gottfried.strasser@tuwien.ac.at (G.S.)

² Austrian Academy of Sciences, Dr. Ignaz Seipel-Platz 2, 1010 Wien, Austria; hermann.detz@tuwien.ac.at

³ TU Wien, Center for Micro and Nano Structures, Floragasse 7, 1040 Wien, Austria; werner.schrenk@tuwien.ac.at

* Correspondence: tobias.zederbauer@tuwien.ac.at; Tel.: +43-1-58801-36215

Received: 31 March 2016; Accepted: 15 April 2016; Published: 20 April 2016

Abstract: This work provides a detailed study on the growth of $\text{Al}_x\text{In}_{1-x}\text{As}_y\text{Sb}_{1-y}$ lattice-matched to InAs by Molecular Beam Epitaxy. In order to find the conditions which lead to high crystal quality deep within the miscibility gap, $\text{Al}_x\text{In}_{1-x}\text{As}_y\text{Sb}_{1-y}$ with $x = 0.462$ was grown at different growth temperatures as well as As_2 and Sb_2 beam equivalent pressures. The crystal quality of the grown layers was examined by high-resolution X-ray diffraction and atomic force microscopy. It was found that the incorporation of Sb into $\text{Al}_{0.462}\text{In}_{0.538}\text{As}_y\text{Sb}_{1-y}$ is strongly temperature-dependent and reduced growth temperatures are necessary in order to achieve significant Sb mole fractions in the grown layers. At 480 °C lattice matching to InAs could not be achieved. At 410 °C lattice matching was possible and high quality films of $\text{Al}_{0.462}\text{In}_{0.538}\text{As}_y\text{Sb}_{1-y}$ were obtained.

Keywords: MBE; QCL; THz; growth; AllnAsSb; antimonides

1. Introduction

InAs is an interesting material for inter-subband devices such as quantum cascade lasers (QCLs) due to its low effective mass, since it is expected to enable higher performance by providing higher gain [1]. In order to exploit the beneficial properties of InAs as the well material, a suitable barrier material is necessary. The commonly used Al(As)Sb material, though enabling excellent results for mid-infrared (MIR) devices [2–5], requires the use of monolayer and sub-monolayer thin barriers for devices designed to emit in the terahertz (THz) regime, due to its very high conduction band offset. The growth of such thin layers is very difficult to control, and to date, no THz laser operation has been shown.

A viable option for the barrier material is the quaternary $\text{Al}_x\text{In}_{1-x}\text{As}_y\text{Sb}_{1-y}$ material, which can be grown lattice-matched to InAs and should have properties tunable from InAs to $\text{AlAs}_{0.16}\text{Sb}_{0.84}$. By choosing an appropriate composition, it would be possible to grow InAs based THz QCLs with a low conduction band offset and therefore easy to control barrier thicknesses.

Reports about the growth of $\text{Al}_x\text{In}_{1-x}\text{As}_y\text{Sb}_{1-y}$ at various compositions can be found in literature, however, most of these works do not specifically study the growth of $\text{Al}_x\text{In}_{1-x}\text{As}_y\text{Sb}_{1-y}$ and hence little information exists on the effect of the various growth parameters on the crystal quality and layer composition. An overview of the compositions and the respective growth temperatures is given in Figure 1. Turner *et al.* [6] and Wilk *et al.* [7] report on the growth $\text{Al}_x\text{In}_{1-x}\text{As}_y\text{Sb}_{1-y}$ with Al mole fractions below 0.20 at growth temperatures (T_g) of 430 °C and 420 °C, while Semenov *et al.* [8] show that compositions with Al mole fractions of up to 0.25 can be grown at a T_g of 450 °C to 500 °C. For the

greatest flexibility when it comes to designing devices employing $\text{Al}_x\text{In}_{1-x}\text{As}_y\text{Sb}_{1-y}$, composition with higher Al mole fractions have to be investigated and conditions have to be found which suit the widest range of compositions. The growth of $\text{Al}_x\text{In}_{1-x}\text{As}_y\text{Sb}_{1-y}$ on GaAs with higher Al mole fractions is reported at a T_g well below 400 °C. Kudo *et al.* [9] studied the incorporation of Sb into $\text{Al}_x\text{In}_{1-x}\text{As}_y\text{Sb}_{1-y}$ with an Al mole fraction of 0.5 at a T_g of 350 °C grown on GaAs. The authors report a high dislocation density, found in a transmission electron microscopy study of the grown material, resulting from the highly lattice-mismatched conditions. It is questionable whether this result is applicable to the growth of $\text{Al}_x\text{In}_{1-x}\text{As}_y\text{Sb}_{1-y}$ on InAs. Wahsington-Stokes *et al.* [10] report on the growth of $\text{Al}_x\text{In}_{1-x}\text{As}_y\text{Sb}_{1-y}$ with an As mole fraction between 0.37 and 0.72 at a T_g between 355 °C and 378 °C on GaSb substrates and report good crystal quality for the grown layers. The influence of the Sb and As beam equivalent pressures (BEP) or the T_g on the quality and composition of the layers is not mentioned.

2. Experiment Section

2.1. Growth Optimization of $\text{Al}_x\text{In}_{1-x}\text{As}_y\text{Sb}_{1-y}$

The lack of information on the growth of $\text{Al}_x\text{In}_{1-x}\text{As}_y\text{Sb}_{1-y}$ with Al mole fractions around 0.5 at a T_g above 400 °C suggests that challenges, possible due to the presence of a miscibility gap [8], arise from such conditions. Since high crystal quality is expected to be achieved at high T_g , the upper limit for the growth of $\text{Al}_x\text{In}_{1-x}\text{As}_y\text{Sb}_{1-y}$ and the dependence of the crystal quality on the T_g have to be investigated.

$\text{Al}_x\text{In}_{1-x}\text{As}_y\text{Sb}_{1-y}$ with an aluminum mole fraction fixed to 0.462, was grown on InAs. The growth rates of AlAs (on InAs) (R_{AlAs}) and InAs (R_{InAs}) were constant for all samples. R_{AlAs} was set to 0.25 monolayers per second (MLs^{-1}) which corresponds to an aluminum BEP 1.3×10^{-7} torr. R_{InAs} was set to 0.29 MLs^{-1} equaling an indium BEP of 4.5×10^{-7} torr. For the comparison of the group V BEPs to other MBE systems, the As_2 flux was calibrated by the (2×4) to (4×2) transition during growth at different temperatures and normalized to 1 MLs^{-1} . A fit to the exponential function $P_{\text{As}_2}(T) = a + b \exp(\frac{T}{c})$ resulted in the parameters $a = 0.531$ torr, $b = 2.14 \times 10^{-14}$ torr, $c = 23.24 \text{ K}^{-1}$. A plot of this experiment can be found in the supplementary material section.

To find the optimum growth conditions, T_g , As_2 BEP (P_{As_2}) and Sb_2 BEP (P_{Sb_2}) were varied. The range of T_g used in this study was 410 °C to 480 °C. Since $\text{Al}_x\text{In}_{1-x}\text{As}_y\text{Sb}_{1-y}$ should be used in heterostructures together with InAs, P_{As_2} is, in principle, dictated by the optimum BEP to grow high quality InAs [11]. In this study, P_{As_2} was varied in order to investigate its influence on the composition of $\text{Al}_{0.462}\text{In}_{0.538}\text{As}_y\text{Sb}_{1-y}$. The growth parameter regions investigated in this study are indicated by the gray shaded areas in Figure 1.

To investigate the influence of growth parameters, a set of samples was grown in a Riber 32 MBE system on indium-bonded n+ InAs (001) wafers. For the group V materials, valved cracking cells were used with the cracking zone temperatures set to 850 °C and 1000 °C to produce As_2 and Sb_2 respectively. For all samples, first the oxide was thermally desorbed under P_{As_2} of 1.5×10^{-5} torr at 510 °C for 20 min. The temperature was then reduced to 480 °C to grow a 150 nm InAs buffer layer to enhance the surface quality after thermal desorption of the oxide. Next, the T_g was adjusted to the desired growth temperature, at which a 150 nm thick $\text{Al}_{0.462}\text{In}_{0.538}\text{As}_y\text{Sb}_{1-y}$ layer and a 5 nm InAs cap, were grown.

All fabricated heterostructures were measured with high resolution x-ray diffraction (HRXRD) to investigate the crystal quality and composition. The As mole fraction (y) in the grown $\text{Al}_{0.462}\text{In}_{0.538}\text{As}_y\text{Sb}_{1-y}$ layers was corroborated by measuring their in-plane and out-of-plane lattice constant in reciprocal space maps around the InAs (224) diffraction peak and applying Vegard's law. Atomic force microscopy (AFM) was used to determine the surface roughness of all samples.

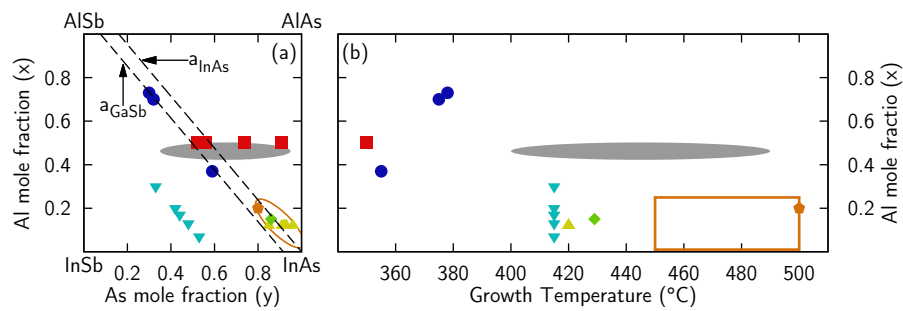


Figure 1. Reports on the growth of $Al_xIn_{1-x}As_ySb_{1-y}$ found in literature. (a) Compositions and (b) their respective T_g . The dashed lines in (a) indicate the compositions of $Al_xIn_{1-x}As_ySb_{1-y}$ which are lattice matched to InAs or GaSb according to Vegard's Law. (◆ condition explicitly mentioned; the range studied is indicated by the outlined areas) Semenov *et al.* [8] grown on InAs; similar results were obtained by Rojas-Ramirez *et al.* [12]; (●) Washington-Stokes *et al.* [10] grown on GaSb; (◆) Turner *et al.* [6] grown on GaSb; (■) Kudo *et al.* [9] grown on GaAs; (▲) Wilk *et al.* [7] grown on InAs; (▼) Sarney *et al.* [13] grown on a lattice-constant shifting AlGaInSb buffer on GaSb; The regions of temperature and composition studied within this work are indicated by the gray shaded areas.

To investigate the incorporation of Sb into $Al_{0.462}In_{0.538}As_ySb_{1-y}$, three series of samples were grown. For each series P_{As_2} and the T_g were kept constant while P_{Sb_2} was varied. P_{As_2} was chosen such that high crystal quality InAs can be grown under the same conditions [11]. The results are summarized in Figure 2a. It shows that with increasing P_{Sb_2} , the rate of Sb incorporation is lowered and a maximum achievable Sb mole fraction is approached asymptotically. Only at a T_g of 410 °C can lattice matching with InAs achieved. An explanation for this behavior may be found in the As-for-Sb exchange reaction found for other mixed group V materials like GaAsSb [14]. Due to its negative enthalpy, this reaction is favored with respect to the reverse reaction and its rate rises with T_g for experiments using As_2 , which is in agreement with our observations.

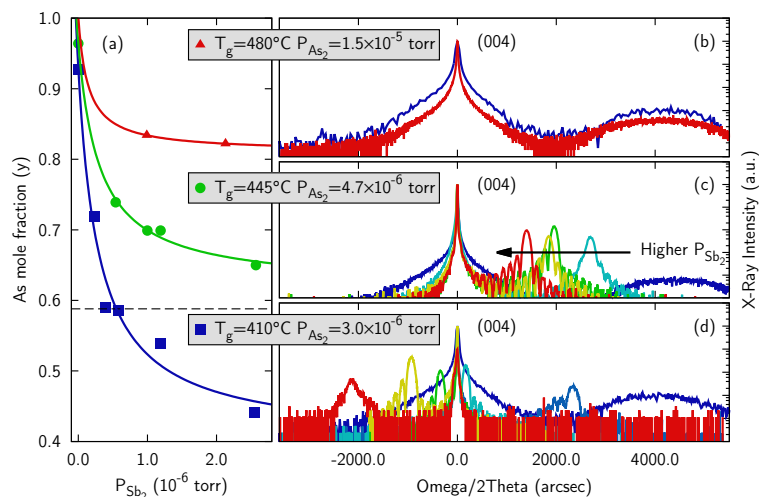


Figure 2. (a) As mole fraction (y) in $Al_{0.462}In_{0.538}As_ySb_{1-y}$ layers with respect to P_{Sb_2} at the values for T_g and P_{As_2} shown in (b–d). Lattice-matching (indicated by the dashed line at $y = 0.588$) is only achieved at 410 °C. high resolution x-ray diffraction (HRXRD) measurements around the InAs (004) diffraction of samples grown at (b) 480 °C, $P_{As_2} = 1.5 \times 10^{-5}$ torr (c) 445 °C, $P_{As_2} = 4.7 \times 10^{-6}$ torr (d) 410 °C, $P_{As_2} = 3.0 \times 10^{-6}$ torr. Fully strained films are found for samples grown at intermediate P_{Sb_2} values at 410 °C and 445 °C. P_{Sb_2} in the subfigures (b–d) given in 1×10^{-6} torr starting from the left most peak: (b): ■ 2.13 ■ 0.99 (c): ■ 2.57 ■ 1.19 ■ 1.00 ■ 0.54 ■ 0.00 (d): ■ 2.55 ■ 1.19 ■ 0.58 ■ 0.39 ■ 0.24 ■ 0.00.

HRXRD measurements, shown in Figure 2b–d, show high crystal quality for P_{Sb_2} between 0.5×10^{-6} torr and 1×10^{-6} torr at 410°C as well as 1×10^{-6} torr and 2.5×10^{-6} torr at 445°C T_g . This is indicated by sharp layer peaks and Pendellösung fringes. At lower P_{Sb_2} , the layer peaks are broadened due to partial relaxation resulting from the high lattice mismatch. At 410°C , even higher P_{Sb_2} also leads to peak broadening. The respective (224) reciprocal space map shows partial relaxation. Strong peak broadening due to partial relaxation was also found for all samples grown at 480°C .

AFM measurements performed on the same heterostructures, shown in Figure 3, confirm these observations. Layers containing very little Sb show crosshatch patterns, a sign of partial relaxation. When the P_{Sb_2} is increased to values between 0.5×10^{-6} torr and 1×10^{-6} torr for a T_g of 410°C and 1×10^{-6} torr and 2.5×10^{-6} torr at 445°C , the surface roughness is dramatically reduced and no sign of crosshatch can be found. At 2.55×10^{-6} torr and a T_g of 410°C , the measurements show an increased surface roughness. Since these conditions cause a 3-D growth mode it is evident that excess Sb_2 has to be avoided at low T_g in order to achieve high crystal quality.

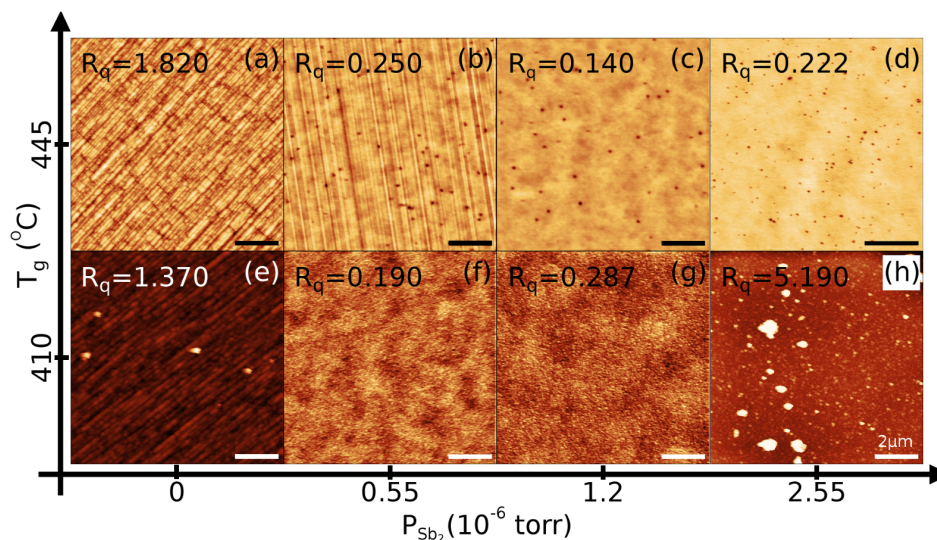


Figure 3. AFM of samples grown at 445°C (a–d) 410°C (e–h) with root mean square roughness values (R_q). P_{Sb_2} is increased left-to-right. Samples grown at low P_{Sb_2} show crosshatch due to the high lattice mismatch (a,b,e). At intermediate P_{Sb_2} , smooth films are obtained (c,d,f,g). At high P_{Sb_2} , high surface roughness is observed (h), scale bar = $2\ \mu\text{m}$. Peak-to-valley values are: (a) 15.9 nm; (b) 3.2 nm; (c) 3.9 nm; (d) 6.4 nm; (e) 23.7 nm; (f) 1.8 nm; (g) 1.5 nm; (h) 44.2 nm.

Although it is convenient to keep P_{As_2} at a value that is optimal for the growth of the InAs throughout the whole growth, it is possible to change the conditions for each layer, since modern As cracking cells are equipped with valves that allow for the quick change of the flux. It could be beneficial to change P_{As_2} to a lower value for the growth of $Al_xIn_{1-x}As_ySb_{1-y}$ in order to achieve a lower As mole fraction in the layer and hereby circumvent the restrictions imposed by the growth of InAs. To investigate the influence of P_{As_2} on the composition of $Al_{0.462}In_{0.538}As_ySb_{1-y}$, a series of samples was grown in which P_{Sb_2} (1×10^{-6} torr and 2.5×10^{-6} torr) and the growth temperature ($T_g = 445^\circ\text{C}$) were kept constant while P_{As_2} was varied. AFM measurements of these samples are shown in Figure 4. From Figure 5a it can be seen that, as expected, decreasing P_{As_2} leads to a lower As concentration (y) in the layer. Figure 5b, shows that the P_{As_2} can only be adjusted within a very small range since too little As_2 leads to a dramatic increase in surface roughness, due a 3-D growth mode (Figure 4c). This behavior is even more pronounced for samples grown at P_{Sb_2} of 2.5×10^{-6} torr (Figure 4a). When P_{As_2} is decreased below $\sim 3 \times 10^{-6}$ torr no epitaxial growth is possible, illustrating that there is a lower limit to the P_{As_2} . This was determined by both a vanishing RHEED pattern during growth and the absence of a layer peak in the HRXRD measurement.

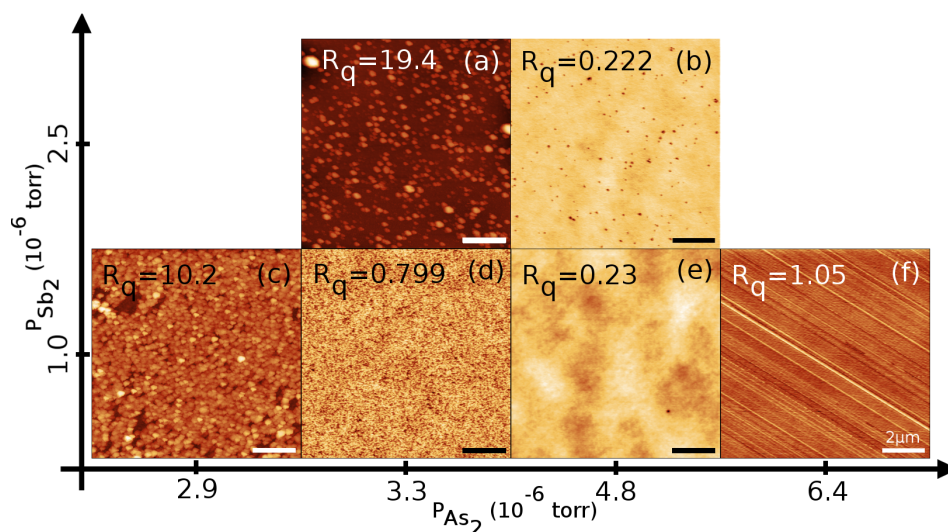


Figure 4. AFM of samples grown at 445 °C at $P_{Sb_2} = 1.0 \times 10^{-6}$ torr and 2.5×10^{-6} torr. P_{As_2} is increased left-to-right. At both values of P_{Sb_2} smooth films were obtained at a P_{As_2} of 4.8×10^{-6} torr. When P_{As_2} is reduced below this value, the roughness is increased dramatically. This is even more pronounced at the higher value of P_{Sb_2} , indicating that this behavior is not caused by a too low total group V flux. It can be concluded that in absence of As, high values of P_{Sb_2} are causing the roughening of the surface. Growing $Al_{0.462}In_{0.538}As_ySb_{1-y}$ at P_{Sb_2} of 1×10^{-6} torr and P_{As_2} of 6.4×10^{-6} torr leads to a high lattice mismatch, which is causes crosshatch and an increased surface roughness. Scale bar = 2 μm . Peak-to-valley values are: (a) 236.2 nm; (b) 6.4 nm; (c) 103.6 nm; (d) 6.9 nm; (e) 2.9 nm; (f) 13.2 nm.

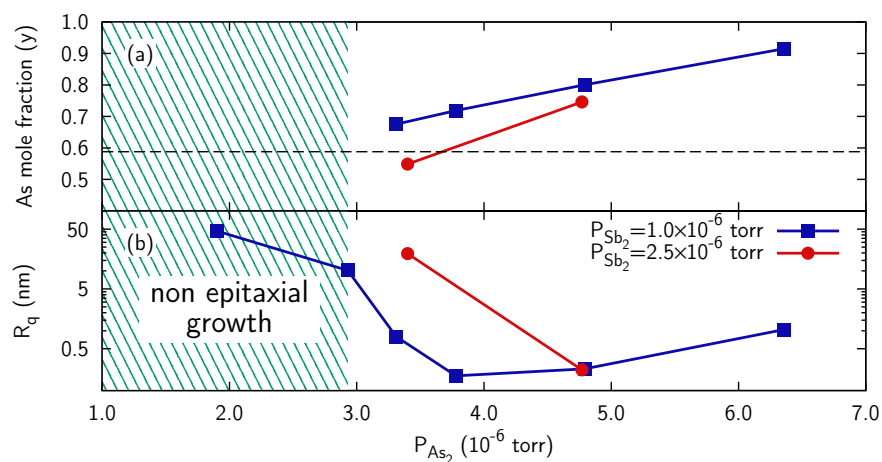


Figure 5. (a) Arsenic mole fraction and (b) root mean square surface roughness (R_q) of $Al_{0.462}In_{0.538}As_ySb_{1-y}$ with respect to P_{As_2} , at two different P_{Sb_2} values and $T_g = 445$ °C. Lattice matching with InAs is indicated by the dashed line in (a). By decreasing P_{As_2} , the As fraction in the grown layer is decreased. The minimum of the surface roughness was found around $P_{As_2} = 4 \times 10^{-6}$ torr. Below $P_{As_2} = 3 \times 10^{-6}$ torr no epitaxial grown is possible under these conditions.

To understand its origin, samples showing high roughness but no cross hatch in the AFM analysis have been inspected by scanning electron microscopy (SEM) and energy dispersive X-ray spectroscopy (EDX). The micrographs of these samples are shown in Figure 6. Figure 6a shows the effect of low P_{As_2} on the surface morphology. The too low As flux on the surface leads to a lower surface mobility of the group III adatoms, breaking the layer-by-layer growth mode and resulting in a rough surface. EDX measurements at different spots of the sample show that the four atom species (Al, In, As, Sb) are equally distributed ($\sigma < 0.5$ at.%). Figure 6b shows the effect of high P_{Sb_2} at low T_g . Similar to Figure 6a

3-D growth was found. Since this sample was grown with excess P_{As_2} , group V deficiency can be ruled out as the source. As for the previous sample, the EDX analysis showed that all four atom species are homogeneously distributed ($\sigma < 0.5$ at.%). Increasing P_{Sb_2} well beyond lattice-matching seems to limit the diffusion length of the group III elements and promote a 3-D growth mode. For both sample (a) and (b) no signs of phase separation due to immiscibility were found and the 3-D morphology seems to be caused by the III/V BEP ratios. High surface roughness was also found for the sample shown in Figure 6c. Unlike for samples (a) and (b) it seems to be due to crystallites with an octagonal base that are well ordered to the substrate. The EDX measurement on this sample shows that the crystallites are rich in antimony while in the surrounding area the composition is close to that found in the HRXRD study. Al and In are homogeneously distributed across the whole sample. This result suggests that $Al_{0.462}In_{0.538}As_ySb_{1-y}$ decomposes into AlInAs and AlInSb under these conditions.

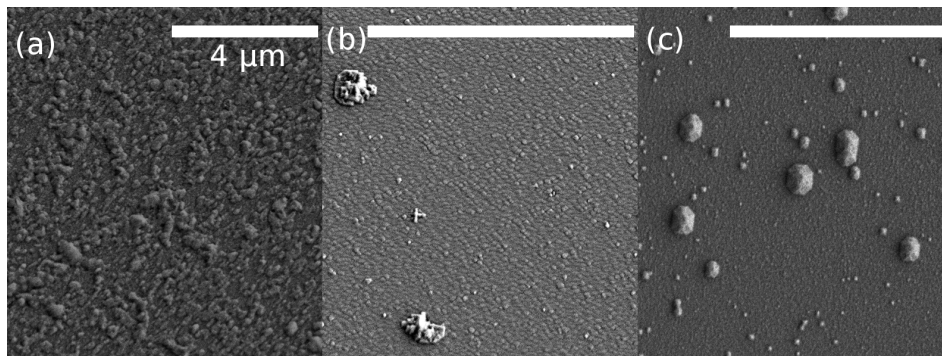


Figure 6. Samples that exhibited high surface roughness but no cross hatch in the AFM analysis have been measured by SEM. (a) corresponds to Figure 4c: $T_g = 445$ °C, $P_{As_2} = 2.9 \times 10^{-6}$ torr, $P_{Sb_2} = 1.0 \times 10^{-6}$ torr. 3-D island growth, caused by a low As_2 coverage of the sample, was found. Energy dispersive X-ray spectroscopy (EDX) measurements show homogeneous distributions of Al, In, As and Sb; (b) corresponds to Figure 3h: $T_g = 410$ °C, $P_{As_2} = 3 \times 10^{-6}$ torr, $P_{Sb_2} = 2.55 \times 10^{-6}$ torr. 3-D island growth, seem to be caused by a too high Sb_2 flux. Al, In, As and Sb are homogeneously distributed according to the EDX analysis; (c) corresponds to Figure 4a: $T_g = 445$ °C, $P_{As_2} = 3.3 \times 10^{-6}$ torr, $P_{Sb_2} = 2.5 \times 10^{-6}$ torr. Octagonally shaped, well order crystallites are found on this samples. The EDX study shows that the crystallites are rich in Sb with respect to the surrounding area. Scale bar = (4 μ m).

Using the information gathered in this study, two samples were grown on a Riber C21 MBE system on freestanding n+ InAs (001) wafers at a T_g of 410 °C. Al mole fractions of 0.25 and 0.53 were chosen and the As_2 BEP was adjusted for high quality InAs. P_{Sb_2} was then adjusted in order to achieve lattice matching with InAs. For both compositions high-quality material was obtained, again confirmed by HRXRD and AFM measurements.

2.2. Low Temperature Growth of InAs Based Inter-Subband Devices

The experimental data presented in this work show that low T_g is necessary in order to achieve high crystal quality for both, InAs and $Al_{0.462}In_{0.538}As_ySb_{1-y}$. Growth performed at very low T_g , however, can lead to low device performance due to a deterioration of the optical properties and interface quality of the grown materials. To ensure that the requirement to grow at low T_g does not prevent the realization of inter-subband devices, InAs-based devices using AlAsSb barriers were designed and grown at a T_g of 400 °C. A quantum cascade detector (QCD) structure with a vertical transition was designed using a semi-classical Monte-Carlo approach. The device was processed into a mesa structure and illuminated through a 45° wedge faced. It showed a peak specific detectivity 2.7×10^7 cm $\sqrt{Hz} W^{-1}$ at 300 K and a center detection wavelength of 4.84 μ m [15]. Moreover, a THz QCL structure based on a 3-well resonant phonon depletion design was grown. Lasing emission at

3.8 THz was observed by applying a magnetic field at liquid helium temperature. This is the first report of laser performance in the THz regime for InAs-based structures [16].

3. Discussions

A summary of all samples used in this study that have been grown at $T_g = 445^\circ\text{C}$ (a) and 410°C (b) is given in Figure 7. In both cases, a large $P_{\text{As}_2}/P_{\text{Sb}_2}$ ratio leads to cross hatch, due to a large lattice mismatch. For a T_g of 445°C , a P_{As_2} below 3.3×10^{-6} torr leads to a rough surface. Roughening was also found for samples grown at a T_g of 410°C for the highest P_{Sb_2} of 2.5×10^{-6} torr. While partial relaxation was found in the reciprocal space map around the InAs (224), the roughening seems to be mainly caused by the high P_{Sb_2} since no sign of cross hatch was found in either EDX or AFM measurements. Growing at higher P_{Sb_2} at a T_g of 445°C results in lower film quality, due to the formation of ordered crystallites with an octagonal base. Since these crystallites were found to be rich in Sb in the EDX analysis, it appears that decomposition, probably due to the miscibility gap of the material occurs under these conditions. A first order approximation, shown as the gray shaded area in Figure 7, was used to locate the region of pressures for which lattice matching can be expected. At a T_g of 445°C this region is close, if not within, the region which leads to decomposition and the formation of Sb rich crystallites. At a T_g of 410°C the region at which lattice matching is expected is far below the region for which the roughening due to high P_{Sb_2} is observed and the growth of lattice-matched high quality material is easily achieved.

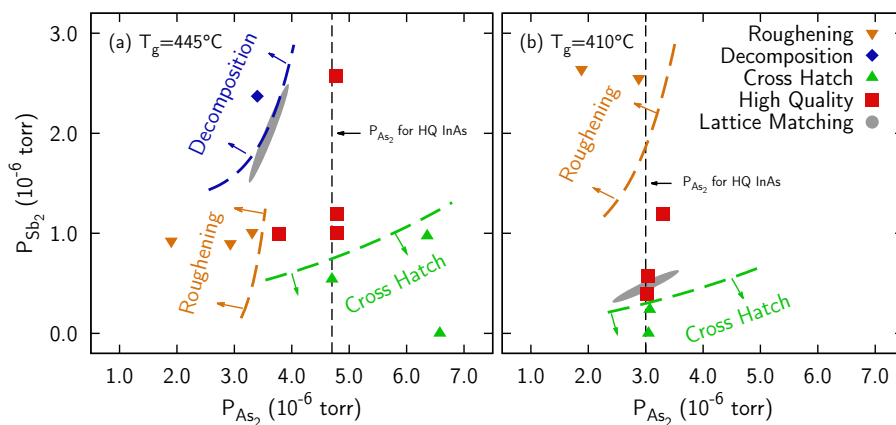


Figure 7. Summary of all samples used in this study that have been grown at $T_g = 445^\circ\text{C}$ (a) and 410°C (b). At both T_g , high $P_{\text{As}_2}/P_{\text{Sb}_2}$ ratios lead to cross hatch due to a large lattice mismatch. For a T_g of 445°C , P_{As_2} below 3.3×10^{-6} torr leads to a rough surface. Growth performed at high P_{Sb_2} leads to the formation of crystallites which suggest that the material is decomposing due to the miscibility gap. At higher values of P_{As_2} high quality material is grown. At this T_g the region in which lattice matching can be achieved is close to the region for which the formation of crystallites is observed. Samples grown at a T_g of 410°C show roughening of the surface at high P_{Sb_2} . At this T_g the region in which lattice matching is possible is far away from the region in which surface roughening was found.

The data presented in this study suggests that a T_g of 445°C is the upper limit for lattice matched growth of $\text{Al}_{0.462}\text{In}_{0.538}\text{As}_y\text{Sb}_{1-y}$. For a stable growth and high quality material, however, it is advised to use even lower T_g . This is even more critical if the conditions for high-quality InAs and $\text{Al}_{0.462}\text{In}_{0.538}\text{As}_y\text{Sb}_{1-y}$ have to be met simultaneously.

4. Conclusions

We investigated the growth of $\text{Al}_{0.462}\text{In}_{0.538}\text{As}_y\text{Sb}_{1-y}$. It was shown that the incorporation of Sb into $\text{Al}_{0.462}\text{In}_{0.538}\text{As}_y\text{Sb}_{1-y}$ is strongly temperature-dependent and that this is determining the upper

limit of the T_g for which lattice matching can be achieved. Moreover, it was found that the quality of the grown material is very sensitive to the used P_{As_2} , and that low pressures, which are necessary to achieve lattice matching, dramatically increase the roughness of the grown layer. Moreover, it was found that the growth of compositions close to lattice matching at a T_g of 445 °C leads to decomposition of $Al_xIn_{1-x}As_ySb_{1-y}$ into AlInAs and AlInSb and the formation of crystallites which significantly decrease in crystal quality. Below this limit, the requirements for the growth of high quality $Al_{0.462}In_{0.538}As_ySb_{1-y}$ and lattice matched growth can be met simultaneously. At a growth temperature of 410 °C, high quality $Al_{0.462}In_{0.538}As_ySb_{1-y}$ layers, confirmed by both HRXRD and AFM measurements, were grown. To ensure that growth at low T_g does not prevent the use of this material for inter-subband devices, two InAs based inter-subband structures, a QCD and a THz-QCL, were grown. The QCD showed a peak specific detectivity $2.7 \times 10^7 \text{ cm } \sqrt{\text{Hz}} \text{ W}^{-1}$ at 300 K at a center detection wavelength of 4.84 μm . For the THz-QCL, we were able to show the first lasing emission in the THz regime, at an emission frequency of 3.8 THz, for InAs-based structures.

Acknowledgments: The authors acknowledge funding by the Austrian Science Fund (FWF): F4909-N23 (NextLite), W1243 (Solids4Fun), F2503-N17 (IRON), as well as support by the Austrian Society for Micro- and Nanoelectronics (GMe). H.D. is an APART fellow of the Austrian Academy of Sciences

Author Contributions: T.Z. conceived and designed the experiments, performed HRXRD, SEM, EDX and AFM measurements and analyzed the data; T.Z. and A.M.A. grew samples and wrote the paper; D.M., H.D. and W.S. configured the MBE for the growth of $Al_xIn_{1-x}As_ySb_{1-y}$; G.S. supervised the study. All authors contributed to scientific discussions and commented on the manuscript.

Conflicts of Interest: The authors declare no conflict of interest.

References

- Ohtani, K.; Ohno, H. InAs/AlSb quantum cascade lasers operating at 10 μm . *Appl. Phys. Lett.* **2003**, *82*, 1003–1005.
- Teissier, R.; Barate, D.; Vicet, A.; Alibert, C.; Baranov, A.; Marcadet, X.; Renard, C.; Garcia, M.; Sirtori, C.; Revin, D.; Cockburn, J. Room temperature operation of InAs/AlSb quantum cascade lasers. *Appl. Phys. Lett.* **2004**, *85*, 167–169.
- Devenson, J.; Teissier, R.; Cathabard, O.; Baranov, A. InAs/AlSb quantum cascade lasers emitting below 3 μm . *Appl. Phys. Lett.* **2007**, *90*, doi:10.1063/1.2714098.
- Devenson, J.; Cathabard, O.; Teissier, R.; Baranov, A. InAsAlSb quantum cascade lasers emitting at 2.75–2.97 μm . *Appl. Phys. Lett.* **2007**, *91*, doi:10.1063/1.2790824.
- Marcadet, X.; Renard, C.; Carras, M.; Garcia, M.; Massies, J. InAs/AlAsSb based quantum cascade lasers. *Appl. Phys. Lett.* **2007**, doi:10.1063/1.2790824.
- Turner, G.W.; Choi, H.K.; Le, H.Q. Growth of InAsSb quantum wells for long-wavelength ($\sim 4 \mu\text{m}$) lasers. *J. Vac. Sci. Technol. B Microelectron. Nanometer Struct.* **1995**, *13*, 699, doi:10.1116/1.588139.
- Wilk, A.; Fraise, B.; Christol, P.; Boissier, G.; Grech, P.; El Gazouli, M.; Rouillard, Y.; Baranov, A.; Joullié, A. MBE growth of InAs/InAsSb/InAlAsSb “W” quantum well laser diodes emitting near 3 μm . *J. Cryst. Growth* **2001**, *227–228*, 586–590.
- Semenov, A.; Solov'ev, V.; Meltser, B.; Terent'ev, Y.; Prokopova, L.; Ivanov, S. Molecular beam epitaxy of AlInAsSb alloys near the miscibility gap boundary. *J. Cryst. Growth* **2005**, *278*, 203–208.
- Kudo, M.; Mishima, T. MBE growth of Si-doped InAlAsSb layers lattice-matched with InAs. *J. Cryst. Growth* **1997**, *175–176*, 844–848.
- Washington-Stokes, D.; Hogan, T.; Chow, P.; Golding, T.; Kirschbaum, U.; Littler, C.; Lukic, R. $Al_xIn_{1-x}As_{1-y}Sb_y$ /GaSb effective mass superlattices grown by molecular beam epitaxy. *J. Cryst. Growth* **1999**, *201–202*, 854–857.
- Ye, H.; Li, L.; Hinkey, R.; Yang, R.; Mishima, T.; Keay, J.; Santos, M.; Johnson, M. MBE growth optimization of InAs (001) homoepitaxy. *J. Vac. Sci. Technol. B Nanotechnol. Microelectron.* **2013**, *31*, doi:10.1116/1.4804397.
- Rojas-Ramirez, J.; Wang, S.; Contreras-Guerrero, R.; Caro, M.; Bhatnagar, K.; Holland, M.; Oxland, R.; Doornbos, G.; Passlack, M.; Diaz, C.; *et al.* $Al_xIn_{1-x}As_ySb_{1-y}$ alloys lattice matched to InAs(100) grown by molecular beam epitaxy. *J. Cryst. Growth* **2015**, *425*, 33–38.

13. Sarney, W.; Svensson, S.; Wang, D.; Donetsky, D.; Kipshidze, G.; Shterengas, L.; Lin, Y.; Belenky, G. AlInAsSb for M-LWIR detectors. *J. Cryst. Growth* **2015**, *425*, 357–359.
14. Losurdo, M.; Capezzuto, P.; Bruno, G.; Brown, A.S.; Brown, T.; May, G. Fundamental reactions controlling anion exchange during mixed anion heterojunction formation: Chemistry of As-for-Sb and Sb-for-As exchange reactions. *J. Appl. Phys.* **2006**, *100*, doi:10.1063/1.2216049.
15. Reiningner, P.; Zederbauer, T.; Schwarz, B.; Detz, H.; MacFarland, D.; Andrews, A.M.; Schrenk, W.; Strasser, G. InAs/AlAsSb based quantum cascade detector. *Appl. Phys. Lett.* **2015**, *107*, doi:10.1063/1.4929501.
16. Brandstetter, M.; Kainz, A.M.; Zederbauer, T.; Krall, M.; Schönhuber, S.; Detz, H.; Schrenk, W.; Andrews, A.M.; Strasser, G.; Unterrainer, K. InAs based terahertz quantum cascade lasers. *Appl. Phys. Lett.* **2016**, *108*, doi:10.1063/1.4939551.



© 2016 by the authors; licensee MDPI, Basel, Switzerland. This article is an open access article distributed under the terms and conditions of the Creative Commons Attribution (CC-BY) license (<http://creativecommons.org/licenses/by/4.0/>).